Tetraoxane Antimalarials and Their Reaction with Fe(II)

Igor Opsenica,[†] Nataša Terzić,[†] Dejan Opsenica,[†] Goran Angelovski,[§,||] Manfred Lehnig,[§] Peter Eilbracht,[§] Bernard Tinant,[‡] Zorica Juranić,[⊥] Kirsten S. Smith,[▽] Young S. Yang,[▽] Damaris S. Diaz,[▽] Philip L. Smith,[▽] Wilbur K. Milhous,[▽] Dejan Doković,[#] and Bogdan A. Šolaja*[,#]

Institute of Chemistry, Technology and Metallurgy, Belgrade, Serbia and Montenegro, Fachbereich Chemie, Organische Chemie I, Universität Dortmund, D-44221 Dortmund, Germany, Laboratoire de Chimie Physique et de Cristallographie, Université Catholique de Louvain, Louvain-la-Neuve, Belgium, National Cancer Research Institute, Belgrade, Serbia and Montenegro, Division of Experimental Therapeutics, Walter Reed Army Institute of Research, Washington, D.C. 20307-5100, and Faculty of Chemistry, University of Belgrade, Belgrade, Serbia and Montenegro

Received September 28, 2005

Mixed tetraoxanes **5a** and **13** synthesized from cholic acid and 4-oxocyclohexanecarboxylic acid were as active as artemisinin against chloroquine-susceptible, chloroquine-resistant, and multidrug-resistant *Plasmodium falciparum* strains (IC_{50}, IC_{90}). Most active **13** is metabolically stable in in vitro metabolism studies. In vivo studies on tetraoxanes with a C(4″) methyl group afforded compound **15**, which cured 4/5 mice at 600 and 200 mg·kg^{-1}·day^{-1}, and 2/5 mice at 50 mg·kg^{-1}·day^{-1}, showing no toxic effects. Tetraoxane **19** was an extremely active antiproliferative with LC_{50} of 17 nM and maximum tolerated dose of 400 mg/kg. In Fe(II)-induced scission of tetraoxane antimalarials only RO$^{\bullet}$ radicals were detected by EPR experiments. This finding and the indication of Fe(IV)═O species led us to propose that RO$^{\bullet}$ radicals are probably capable of inducing the parasite's death. Our results suggest that C radicals are possibly not the only lethal species derived from peroxide prodrug antimalarials, as currently believed.

Introduction

Malaria infects 300−500 million people each year, affecting tropical areas of the world with a death toll of up to two million.[1] Of the four human varieties of malaria, *Plasmodium falciparum* is the most dangerous, accounting for half of all clinical cases of malaria and 90% of deaths from the disease. Increased resistance to standard antimalarial drugs such as chloroquine complicates the treatment of infected individuals. Therefore, development of highly efficacious and cost-effective treatments is urgently needed. The success and usefulness of peroxide antimalarials of the 1,2,4-trioxacyclohexane class, or trioxanes, such as artemisinin and its derivatives, have opened new possibilities for treating parasitemia. The 1,2,4,5-tetraoxacyclohexanes[2] are a class of compounds with similar activity to that of artemisinin-derived antimalarials that are currently being investigated for their antimalarial activity.

In addition to bis-steroidal tetraoxanes,[2b,3] a significant number of dicyclohexylidene tetraoxanes have been synthesized, and their antimalarial activity has been evaluated in vitro and in vivo.[4] However, the structures of both above-mentioned tetraoxane types that could be explored were limited by the mode of their synthesis: only bis compounds could be obtained directly from the corresponding ketones. Recent syntheses of mixed tetraoxanes have opened new possibilities for the controlled preparation of this class of promising antimalarials.[5,6]

Until now, steroidal mixed tetraoxanes possessing only a 4″-alkyl/aryl substituent have been synthesized.[5,7] Here, we report the synthesis and the results of in vitro biological evaluation of mixed tetraoxanes derived from cholic acid and 4-oxocyclohexanecarboxylic acid, with the aim to investigate the influence of C(O)X substituents (wherein X is OH, OR, NH_2, NHR) on antimalarial activity of mixed tetraoxanes having the general structure **I**, Chart 1. In addition, we report the in vivo screening results of mixed tetraoxanes of general structure **II**.

Chart 1

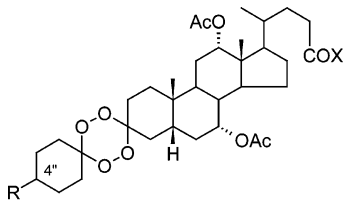

I : R = C(O)X

II : R = CH_3, H

Previous work showed that steroidal tetraoxanes inhibit cancer cell proliferation at micromolar and submicromolar levels through an apoptotic mechanism.[3,7] It was also discovered that tested compounds exhibit high selectivity index (SI) when their toxicity against healthy cells was compared to respective antimalarial or antiproliferative activity against tumor cells.[3a,5] Accordingly, we investigated the antiproliferative activity of mixed tetraoxanes with general structures **I** and **II** against both tumor and normal cell lines.

In addition to biological evaluation, which confirmed the pronounced antimalarial activity of the examined class of peroxides, we investigated the mechanism of action of selected mixed tetraoxanes using model experiments. It is currently believed that peroxide antimalarials selectively kill the *P. falciparum* parasite by heme[8] or non-heme[9] iron-generated carbon-centered radicals. By use of radical scavengers in the model experiments, it has been shown that after initial Fe(II)-

* Corresponding author. Mailing address: Faculty of Chemistry, University of Belgrade, Studentski trg 16, P.O. Box 158, YU-11001 Belgrade, Serbia and Montenegro. Phone: +381-11-63-86-06. Fax: +381-11-63-60-61. E-mail: bsolaja@chem.bg.ac.yu.

[†] Institute of Chemistry, Technology and Metallurgy.

[§] Universität Dortmund.

[||] Current address: Max-Planck Institute for Biological Cybernetics, Tübingen, Germany.

[‡] Université Catholique de Louvain.

[⊥] National Cancer Research Institute.

[▽] Walter Reed Army Institute of Research.

[#] University of Belgrade.

10.1021/jm050966r CCC: $33.50
Published on Web 06/08/2006

Scheme 1

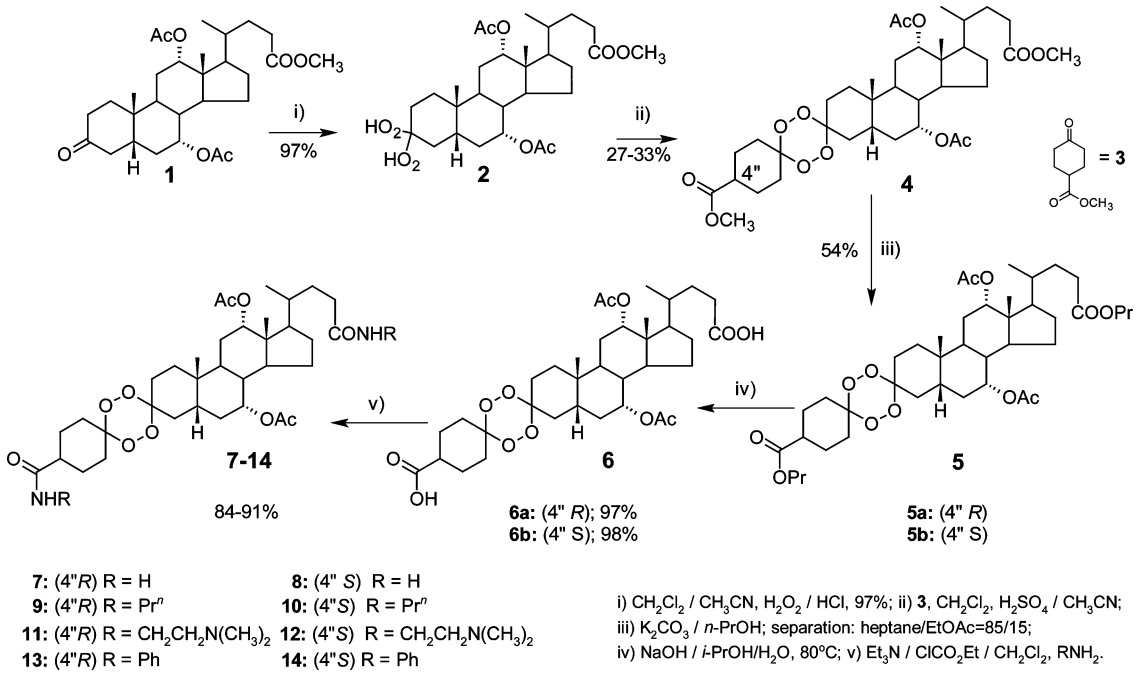

induced O-radical generation, 1,5-H shift, or β-scission, occurs to afford a C-centered radical, which may alkylate heme[10] or other biological molecules in the proposed lethal event. It has also been proposed that both red blood cells (RBC) and parasite membranes are subject to fatal lipid peroxidation in the presence of artemisinin and heme.[11] FP−Fe(II)/FP−Fe(III) (heme/hematin) has been found to accumulate in the parasite's food vacuole (FV) prior to hemozoin formation, and since non-heme iron is speculated to exist in the parasite's cytosol,[9] it is proposed that C-centered radicals may initiate the lipid peroxidation as well.[8,11] However, no evidence for the formation of alkoxy radicals as possible chain initiators has yet been observed.

Chemistry

Mixed tetraoxanes **5**−**14** were prepared (Scheme 1) using the procedure described in ref 5. Coupling of *gem*-dihydroperoxide **2** to prochiral ketone **3** afforded the mixture of C(4″) epimers **4**. The said mixture of methyl esters **4** could not be resolved on SiO_2 or on RP-18 column; however, upon transesterification of **4** (*n*-PrOH/K_2CO_3), the obtained mixture of *n*-propyl esters **5** was successfully resolved on a SiO_2 column affording **5a** and **5b** in 54% combined yield. The esters **5a** and **5b** were selectively hydrolyzed into acids **6a** and **6b**, respectively, which were further transformed into two series of the corresponding amides **7**−**14**. The overall yield of amides in each series starting from *gem*-dihydroperoxide **2** was ca. 13%. The obtained compounds have been fully characterized using standard spectroscopic methods.

The substitution pattern at C(4″) could not be determined on the basis of NMR spectral data; however, the problem was solved using X-ray crystallographic structural analysis of the monocrystal of tetraoxane **8**. The configuration at C(4″) in **8** was found to be *S* (Figure 1); consequently, tetraoxanes **5b**, **6b**, **10**, **12**, and **14** were assigned to the same, (4″*S*)-series, while the diastereomeric (4″*R*)-series consists of compounds **5a**, **6a**, **7**, **9**, **11**, and **13**.

The asymmetric part of the unit cell of **8** consists of four tetraoxane molecules and a large number of solvent molecules: one heptane, three ethyl acetate, four water, one acetone, and one methanol molecule were identified and refined. There are probably other cocrystallized solvent molecules but with low occupation factors; this explains the high number of peaks with density around 0.5−0.7 e A^{-3} in the residual density. It is also the reason for the relatively high *R* indices.

The four tetraoxane molecules have a similar geometry; only slight differences in the orientation of the extremities of the side chains are observed. For example, the torsion angle C(22)−C(23)−C(24)−O(25) is 76°, −70°, 75°, and 30° for molecules 1−4, respectively. All the NH_2 groups are involved in the hydrogen bonding net.

Antimalarial Activity

The synthesized tetraoxanes **5**−**14** were screened in vitro against three *P. falciparum* strains—D6 (chloroquine-susceptible), W2 (chloroquine-resistant, susceptible to mefloquine), and TM91C235 (Thailand), a multidrug-resistant strain—following the protocol given in ref 3a. The results shown in Table 1 clearly indicate that members of (4″*R*)-series are much more active than corresponding (4″*S*)-epimers, demonstrating significant dependence of the activity on a minor structural change (vide infra). The overall activity of the compounds **6a**, **7**, **9**, and **11** is lower than that of the corresponding (4″*R*)-methyl series (Table 2); however, ester **5a** and anilide **13** appear to be highly active antimalarials. Both compounds exert pronounced activity against highly resistant W2 and TM91C235 strains, with in vitro activity (at the IC_{50} and, more importantly, at the IC_{90} level[12]) of both compounds comparable to or better than artemisinin.

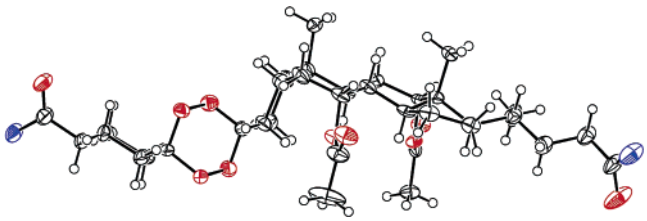

Figure 1. Ortep plot of tetraoxane **8**. Carbons are represented as partially filled elipsoids, hydrogens as unfilled circles, oxygens in red, and nitrogens in blue.

Table 1. In Vitro Antimalarial Activities of Tetraoxanes **5**−**14** against *P. falciparum* D6,[a] W2,[b] and TM91C235[c] Strains

	IC_{50} (nM)			IC_{90} (nM)		
compd	D6	W2	TM91C235	D6	W2	TM91C235
			(4″*R*) Series			
5a	6.7	9.0	8.8	9.4	17.4	18.0
6a	98.3	135.4	134.6	147.1	155.6	256.6
7	11.0	17.1	11.8	17.3	34.4	56.7
9	10.5	18.1	14.9	17.8	39.6	63.2
11	75.6	112.9	81.4	94.1	126.2	109.7
13	6.2	11.4	8.1	11.3	20.8	19.2
artemisinin[d]	9.0	6.7	13.04	12.8	11.5	17.4
chloroquine[e]	13.7	349.4	144.9	17.6	491.5	268.8
			(4″*S*) Series			
5b	30.3	41.4	42.2	47.4	83.5	75.8
8	119.1	120.8	167.6	196.3	264.6	249.2
6b	>300	>300	>300	>300	>300	>300
8	119.1	120.8	167.6	196.3	264.6	249.2
10	38.5	58.3	52.3	56.0	78.0	126.8
12	127.9	132.3	145.2	187.4	166.6	159.7
14	29.6	52.9	42.8	44.5	74.2	86.6
mefloquine[e]	10.5	3.1	16.4	21.7	8.4	65.7

[a] *P. falciparum* African D6 clone. [b] *P. falciparum* Indochina W2 clone. [c] *P. falciparum* multidrug resistant TM91C23 strain (Thailand). [d] Average of greater than eight replicates. [e] Control drugs.

Here, we also present the in vivo activity for five compounds synthesized earlier[5] (**15**−**19**, Chart 2). These five compounds were tested in mice infected with *P. berghei* using a modified Thompson test. The mice were infected on day 0, and the tested compounds were administered orally on days 3, 4, and 5 postinfection.

In general, the tested compounds were orally active and cured the infected mice at high doses, while being less active at lower applied doses of 50 mg·kg^{-1}·day^{-1} (Table 2). The (4″*R*)- and (4″*S*)-tetraoxane amides (**15** and **17**) showed higher in vivo activity as compared to their carboxylic acid analogues (**16** and **18**).

Compound **15** cured 4/5 mice at the doses 600 and 200 mg·kg^{-1}·day^{-1} for 3 days, while being moderately active at doses of 50 mg·kg^{-1}·day^{-1}. Its epimer **17** cured all mice at high doses (600 mg·kg^{-1}·day^{-1}) and only one at 200 mg·kg^{-1}·day^{-1}. Both epimers were equally active at 50 mg·kg^{-1}·day^{-1} (2/5 mice cured) with approximately the same survival time.

Chart 2

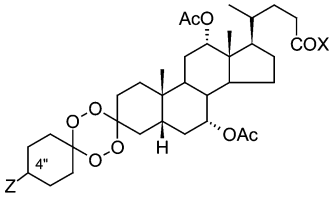

15: X = NH_2, Z = (*R*) CH_3

16: X = OH, Z = (*R*) CH_3

17: X = NH_2, Z = (*S*) CH_3

18: X = OH, Z = (*S*) CH_3

19: X = *n*-Pr, Z = H

The activity of these two compounds is currently being reexamined, and they will be scrutinized in detail. The propyl amide **19**, which was also effective at high doses, showed no cure at 50 mg·kg^{-1}·day^{-1}. No observable toxic effects were observed with any of the compounds screened in vivo. The in vivo activity of tetraoxanes **15**−**19** appears to be less prominent as compared to current peroxide antimalarial drug candidates,[8] trioxolanes,[13] and trioxane dimers.[14]

Antiproliferative Activity

Five compounds possessing the C(4″)-C(O)X group (**5a**, **6a**, **7**, **11**, and **13**; all C(4″*R*)-series)) were chosen by NIH−NCI for in vitro screening in a panel of 60 human tumor cell lines starting at a concentration of 10^{-4} M of the investigated compound.[15] Selected results, given in Table 3, indicate that the tested tetraoxanes are strong antiproliferatives with GI_{50} values within 50 nM to 2 μM. In addition to showing pronounced cytotoxicity against a specific melanoma cell line (LOX IMVI; average LC_{50} ca. 11 μM), the compounds were also very potent against UO-31 renal cancer cells. The most active of tested C(4″)-C(O)X compounds was tetraoxane **13**, which had submicromolar activity against UO-31 cells (LC_{50} = 0.51 μM, Table 3, Figure 2a).

The antiproliferative screening of tetraoxanes **15**−**19** in the same test confirmed that steroidal tetraoxane amides are stronger

Table 2. Activity of Tetraoxanes **15**−**19** against *P. berghei* in Vivo

	in vitro activity IC_{50} (nM)[a]		in vivo activity (p.o.)[b]			
compd	D6	W2	mg·kg^{-1}·day^{-1}	mice dead/day died	mice alive day 31/total	survival time (days)[c]
15 (4″*R*)	1.17	0.58	600	1/26	4/5	29.2
			200	1/16	4/5	27.2
			50	1/12, 1/16, 1/19	2/5	21.4
16 (4″*R*)	1.53	0.98	600	1/25	4/5	29.0
			200	1/18, 1/19, 1/27	2/5	24.8
			50	3/10, 1/13, 1/18	0/5	12.2
17 (4″*S*)	20.01	14.10	600		5/5	30
			200	1/15, 1/16, 1/22, 1/26	1/5	21.8
			50	2/13, 1/20	2/5	21.2
18 (4″*S*)	31.10	17.74	600	3/17, 1/19	1/5	20.0
			200	1/11, 1/19, 1/23	2/5	22.6
			50	4/10, 1/11	0/5	10.2
19	14.76	6.80	600	1/20	4/5	28.0
			200	1/20, 2/21	2/5	24.4
			50	1/7, 2/10, 1/18, 1/26	0/5	14.2
chloroquine[d]	13.76	185.38	4	1/17, 1/21	3/5	25.6
			2	2/10, 1/11, 1/16, 1/17	0/5	12.8
infected controls[e]			0	1/9, 4/10	0/5	

[a] For the sake of better comprehension, we have included the in vitro results published in ref 5. [b] Groups of five *P. berghei* (KBG 173 strain) infected CD-1 mice were treated on days 3, 4, and 5 postinfection with tetraoxanes suspended in 0.5% hydroxyethylcellulose−0.1% Tween 80. Mice alive on day 31 with no parasites in a blood film are considered cured. [c] Including cured mice. [d] Control drug. [e] All noninfected age controls survived (5/5).

Table 3. In Vitro Antiproliferative Activities of Tetraoxanes **5**−**13** and **15**−**19** (μM, after 48 h; Selected Data)

compd	cell line		GI_{50}[a]	TGI[b]	LC_{50}[c]
5a	melanoma	LOX IMVI	1.09	2.74	6.91
	ovarian cancer	IGROV1	1.99	6.16	>100
	renal cancer	UO-31	1.15	2.44	5.19
6a	renal cancer	UO-31	1.74	3.65	7.66
7	melanoma	LOX IMVI	1.85	3.95	8.42
	renal cancer	786-0	1.69	3.70	8.08
11	CNS cancer	SF-539	1.47	2.99	9.93
	melanoma	LOX IMVI	1.18	2.82	19.9
		SK-MEL-28	1.92	11.3	37.0
	ovarian cancer	IGROV1	0.90	2.62	13.4
13	non-small-cell lung cancer	EKVX	0.90	>100	>100
	melanoma	LOX IMVI	0.37	1.69	7.15
	renal cancer	786-0	0.45	14.2	67.9
		UO-31	0.05	0.19	0.51
15	non-small-cell lung cancer	EKVX	1.01	2.35	5.49
		HOP-62	1.47	2.96	5.96
	colon cancer	COLO 205	1.56	3.19	6.52
	CNS cancer	U251	1.78	3.78	8.06
	ovarian cancer	IGROV1	1.54	3.07	6.14
	renal cancer	ACHN	1.80	3.88	8.35
		UO-31	1.56	3.08	6.11
17	non-small-cell lung cancer	EKVX	1.43	2.78	5.41
		HOP-62	1.07	2.31	4.98
	colon cancer	COLO 205	1.69	3.12	5.76
		HCT-15	1.71	3.43	6.86
	CNS cancer	SNB-75	1.98	4.05	8.28
	melanoma	SK-MEL-2	1.71	3.20	6.01
		UACC-62	1.85	3.99	8.59
	ovarian cancer	IGROV1	0.49	1.84	4.95
	renal cancer	ACHN	1.50	2.93	5.73
		UO-31	1.26	2.64	5.50
	prostate cancer	PC-3	1.97	4.29	9.31
		DU-145	1.82	3.26	5.85
16	leukemia	SR	1.63	3.82	8.92
18	non-small-cell lung cancer	EKVX	1.45	2.90	5.78
		HOP-62	1.64	3.49	7.40
	colon cancer	COLO 205	1.98	4.40	9.78
	ovarian cancer	IGROV1	1.40	2.76	5.43
	renal cancer	UO-31	1.50	3.00	6.02
19	leukemia	RPMI-8226	1.28	3.47	9.37
	non-small-cell lung cancer	HOP-62	0.44	1.72	5.40
		NCI-H23	0.61	1.99	4.64
		NCI-H460	0.18	0.59	2.60
	colon cancer	COLO 205	1.77	3.72	7.82
	CNS cancer	SF-268	1.57	3.90	9.68
	ovarian cancer	IGROV1	0.19	0.46	1.36
	renal cancer	ACHN	1.34	2.62	5.12
		CAKI-1	0.18	0.40	0.91
		TK-10	1.67	3.62	7.84
		UO-31	<0.01	<0.01	0.017

[a] 50% growth inhibitory activity. [b] Total growth inhibition. [c] Concentration of the compound at which 50% of the cells are killed.

antiproliferatives than corresponding acids (Table 3, **15** and **17** vs **16** and **18**; only selected data falling within $GI_{50} < 2$ μM and $LC_{50} < 10$ μM are presented). Based on available data, the influence of stereochemistry at C(4″) cannot be extracted. However, the *n*-propyl amide **19** appeared to be the most potent antiproliferative tetraoxane tested so far. It is most active against ovarian and renal cancer cell lines. The compound is also highly specific against renal UO-31 cancer cells (Figure 2b) with $LC_{50} = 17$ nM (log $LC_{50} = -7.78$; MG-MID $= -4.47$; mean graph midpoint).

The observed trend of antiproliferative activity adds to our previous observations on the selectivity of steroidal tetraoxanes against UO-31 cancer cells.[3,7]

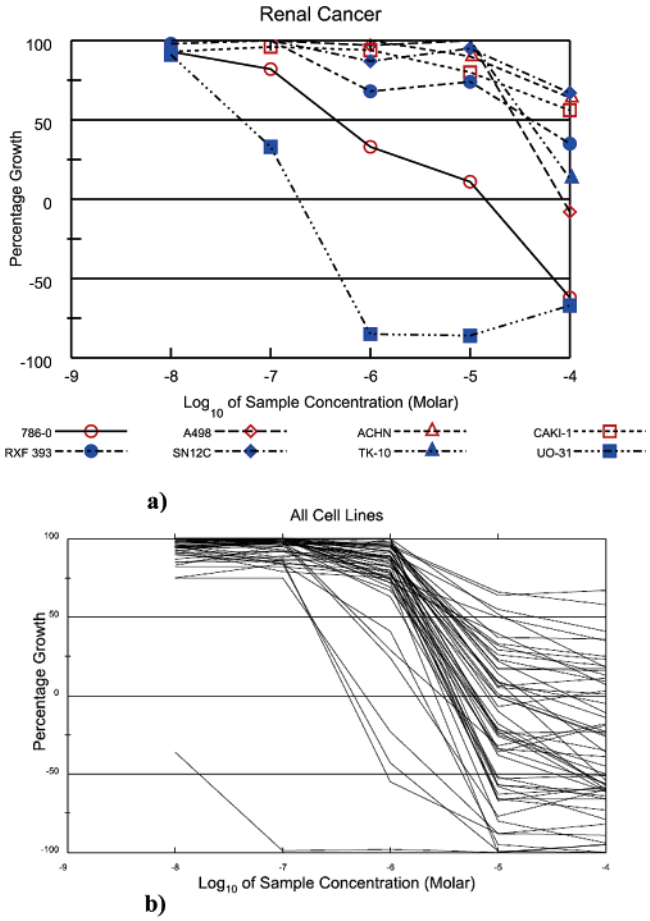

Figure 2. Percentage growth of (a) renal cancer cell lines 48 h after being exposed to tetraoxane **13** and (b) all cancer cell lines 48 h after being exposed to tetraoxane **19**.

Metabolic Profiling

In addition, in vitro metabolism studies were performed on **7**, **11**, and **13** to assess the bioavailability of drug candidates after oral administration. Metabolic stability assays were done using human and mouse liver microsomes to help predict the hepatic microsomal intrinsic clearance ($CL_{int,in\ vitro}$) of the drug candidates in relevant species. The data showed that compounds **11** and **13** were metabolically stable, with half-lives greater than 120 min. Stable compounds were defined as having half-lives of >120 min or $CL_{int} < 0.60$ mL/(min·g). Compound **7** was metabolically unstable, with half-lives of 21 and 38 min and calculated CL_{int} values of 3.40 and 1.59 mL/(min·g) in human and mouse liver microsomes, respectively. Metabolite identification experiments were also done upon incubation with human, mouse, rat, and rhesus monkey microsomes. As expected from stability experiments, no metabolites were formed after 1 h incubation of compounds **11** and **13** with microsomes at 37 °C. For **7**, the two major products of metabolism in all four species were the same hydroxylated and dihydroxylated species. The MS/MS fragmentation of the parent compound and putative metabolites were used in combination with the no-NADPH control experiments to confirm the assignment of peaks as metabolites. MS/MS fragmentation of **7** showed prominent fragment ions at $[MH - 60]^+$ and $[MH - 120]^+$, corresponding to the sequential loss of the two acetate groups, as well as several unassigned fragments at $[MH - 141]^+$, $[MH - 201]^+$, and $[MH - 243]^+$. The hydroxylated metabolite fragmented in a fashion similar to the parent, with the +16 modification remaining on each fragment until its lowest *m*/*z* fragment of $[MH - 261]^+$.

Chart 3

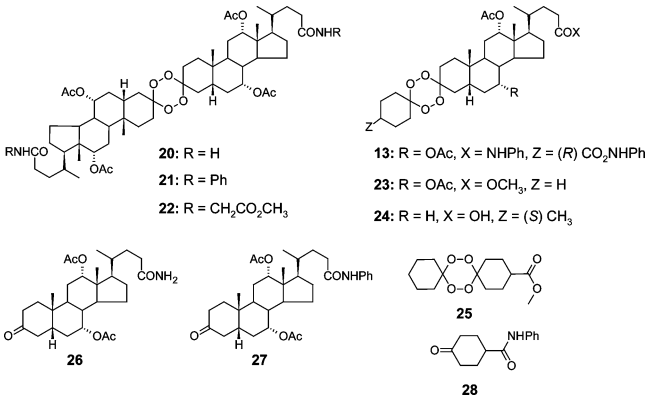

The dihydroxylated metabolite showed only two major fragment ions corresponding to the loss of the acetates. The position of hydroxylation could not be definitively determined.

Reaction with Fe(II)

As previously mentioned, it is accepted that trioxanes and other endoperoxides exert their mode of action by C-radical generation. It is also implied,[13] and recently demonstrated,[16] that C-radicals are generated from ozonides. To examine the reported[17,18] C-radical generation on our tetraoxanes with confirmed antimalarial activity, we have studied their reaction with Fe(II) species using the reaction conditions reported by others.[19,20]

Isolation of Products. Bis-steroidal tetraoxanes **20** and **21** (Chart 3) from our stock,[21] as well as mixed tetraoxane **13**, were subjected to Fe(II)-induced O−O bond scission in acetonitrile ($FeCl_2 \cdot 4H_2O$, 2 equiv[22]) at rt. After workup and purification the following products were isolated: **26**[3a] (from **20**, 95−97%, done in triplicate), **27** (from **21**, 94%), and **27** (84%) and **28** (96%) (both from **13**). In addition, we have performed qualitative experiments to test the reactivity of tetraoxanes. Compound **23** was mixed with $FeCl_3 \cdot 6H_2O$ (2 equiv) in acetonitrile for 5 days affording no reaction; however, upon addition of cysteine (2 equiv) to the same reaction mixture, the reaction immediately started affording ketones (in the blank probe, it was shown that cysteine does not react with **23**). We have also found that a catalytic amount of Fe(III) (ca. 10% of $FeCl_3$), combined with **23** and cysteine (2 equiv), is sufficient to consume all of the tetraoxane yielding ketones (not isolated quantitatively, but confirmed by careful TLC analysis). In analogous experiments using a hemin (as the dimethyl ester)/cysteine system, we were able to observe only ketones as products. Thus, only ketones were detected as products of tetraoxane Fe(II)-induced reductive scission.

EPR Experiments. To detect the reaction species generated during Fe(II)-induced decomposition, tetraoxanes of various types—**22**,[3b] **23**,[5] **24**,[23] and **25**[24]—were combined with $FeCl_2 \cdot 4H_2O$ in the presence of O- and C-radical nitrone spin traps, 5,5-dimethyl-1-pyrrolidine *N*-oxide (DMPO)[25,26] and 5-(diethoxyphosphoryl)-5-methyl-1-pyrrolidine *N*-oxide (DEPMPO).[27] Strong EPR signals appeared within 5−6 min (Figure 3), and the results given in Table 4 indicate that only RO• radicals were generated.[28] For possible structures of R, see Scheme 2.

Fe(IV)═O Species. The high-valent iron-oxo species Fe(IV)═O is postulated to be the intermediate in artemisinin Fe(II) reductive cleavage, as shown by hexamethyl Dewar benzene (HMDB) isomerization into hexamethylbenzene (HMB)[29] and evidenced by IR analysis.[30] Using experimental conditions

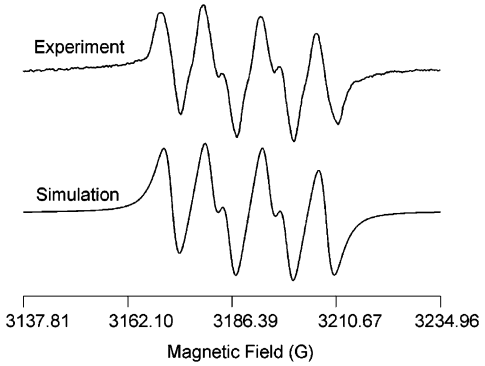

Figure 3. EPR spectrum of DMPO-•OR radical obtained by carrying Fe(II)-induced reductive scission of mixed tetraoxane **22**.

Table 4. EPR Parameters of the Radicals Generated in the Reaction of Tetraoxanes with $FeCl_2$ in the Presence of DMPO or DEPMPO in Acetonitrile

compd	spin trap	*a*(N), G	*a*(H), G	*a*(P), G
22	DMPO	13.4	9.2	
23	DMPO	13.5	8.2	
24	DEPMPO	13.49	8.53	48.90
25	DEPMPO	13.83	8.77	48.90

Scheme 2. Proposed Mechanism for Fe(II)-Induced Tetraoxane Decomposition into Ketones and Fe(IV)═O

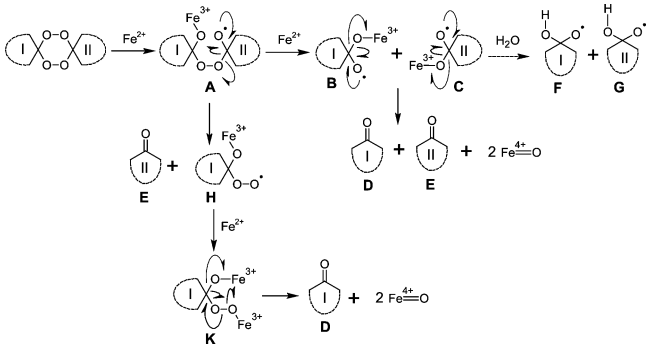

similar to the ones given in ref 29, we exposed tetraoxane **25** to reductive peroxide bond scission, using $FeCl_2 \cdot 4H_2O$ in CH_3CN as the Fe(II) source, in the presence of HMDB. After completion of the reaction (2 equiv of $FeCl_2 \cdot 4H_2O$ needed), GC-MS analysis revealed the formation of two ketones as products (cyclohexanone and methyl 4-oxocyclohexanecarboxylate), together with starting HMDB and the product of rearrangement thereof, HMB, Figure 4. Thus, from this experiment, we conclude that an Fe(IV)═O species is generated during this process.

Discussion

The antimalarial activity of compounds with general structures **I** and **II**, presented in Table 1, clearly indicates that the C(4″*R*)-C(O)X series is significantly more active than the respective epimeric one. This finding is in line with our previous results obtained with C(4″)-methyl (Table 2, ref 5), ethyl,[5] and C(4″)-phenyl[7] mixed tetraoxanes substituted at the cyclohexylidene ring. The observation is also consistent with docking experiments using heme and two epimeric C(4″)-methyl-substituted mixed tetraoxanes, which revealed an energy difference of the two docked structures of 33.5 kcal/mol,[31] in favor of the more active C(4″*R*)-series. It is important to note that the observed trend holds for in vitro and in silico results; however, it was not confirmed by in vivo results.

The acids of both series (**6a** and **6b**) are less active than primary and secondary amides (Tables 1 and 3), thus extending

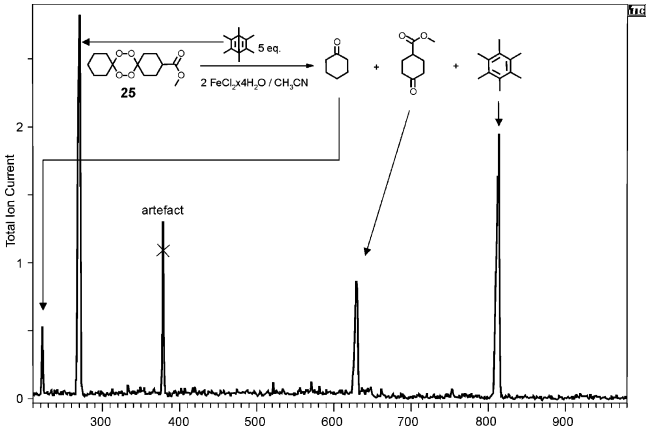

Figure 4. Reaction of tetraoxane **25** with Fe(II) in the presence of HMDB−GC chromatogram of Et_2O extract of crude reaction mixture. For details, see Experimental Procedures section.

our previous findings[3,5,7] to the C(4″)-C(O)X series. The said in vitro observations are for the first time supported by in vivo results presented in Table 2. Thus, tetraoxane **15** is more active at lower administered doses than its carboxylic congener **16** and has a noticeably longer survival time (Table 2). The same holds for the epimeric amide/acid pair, **17**/**18**.

The initial RO• radicals obtained by Fe(II)-induced decomposition of artemisinin,[32] arteflene,[26] and ozonides[13,16] at room temperature obviously undergo C−C bond scission or 1,5-H shift at a greater rate[30b,33] than they react with radical scavengers.[34] In the current investigation, mechanistic studies revealed that tetraoxanes of various types (bis-steroidal (**20**−**22**), mixed tetraoxanes containing a steroid moiety (**13**, **23**, **24**), and simple dicyclohexylidene tetraoxane **25**) generate RO• radicals that do not further rearrange into C-radicals, as evidenced by EPR-detected DMPO-•OR and DEPMPO-•OR spin-trapped adducts (both DMPO and DEPMPO are O− and C-radical nitrone spin traps) and by isolation of ketone products (84−97%) from the reaction mixture. Since the obtained result is not in accordance with Wu's isolation of a C-radical adduct obtained upon reductive scission of simple biscyclohexylidene tetraoxane (Fe(II) source, cysteinate-iron(II) chelate, THF/H_2O, 38−40 °C, overnight),[18] we monitored (EPR, DMPO) the reaction of **23** with $FeCl_2$ for 22 h until complete decay of EPR signal (see Supporting Information). Only the DMPO-•OR signal was visible. For comparison, submitting geminal dihydroperoxide **2** to the same reaction conditions ($FeCl_2 \cdot 4H_2O$, DMPO, CH_3CN) enabled us to detect DMPO-•OR and DMPO-•R spin-trapped adducts (86:14 ratio), confirming that DMPO is a good C-radical nitrone spin trap under our reaction conditions.

Despite discrepancies with Wu's work, our results lead us to propose that tetraoxanes exert their activity by delivering RO• radicals to the parasite thus possibly bringing about its death. In addition to detecting the reaction species formed during O−O Fe(II)-induced scission, we have found the evidence for Fe(IV)═O formation during the decay of initially formed RO• radicals into isolated ketone products, as shown by HMDB → HMB rearrangement.

As for the mechanism of formation of ketones from tetraoxanes discussed here (Scheme 2), we propose two probable pathways comprising the consumption of 2 equiv of ferrous salt, formation of an "alkoxy" radical, occurrence of a high-valent iron-oxo intermediate, and formation of corresponding ketones.[35] Presently, we cannot propose the structure of R in the RO•-spin trap adduct; however, the additional information could be obtained by the analysis of the tetraoxane−heme docked structures of two epimeric tetraoxanes differing in antimalarial activity.[31] It was reported that a more active tetraoxane requires 7.31 kcal mol^{-1} less energy for scission of one of its peroxide bonds (less hindered, α O−O bond, steroid assignation), thus indicating the inequality of the two peroxide bonds in the docked structure with heme. This would suggest that the initial Fe(II)-induced O−O bond scission in tetraoxanes is not random but is structure-driven and includes the stereochemical factors,[17] a situation not encountered with monoperoxide antimalarials.

Table 5. Comparison of Antimalarial and Antiproliferative Activity to Cytotoxicity of Tetraoxanes **13** and **19**

	IC_{50} (μM)					LC_{50} (μM)
compd	PBMC	VERO	D6	W2	TM91C235	UO-31
13	>200		0.006	0.011	0.008	0.51
(SI,[a] PBMC)			(>33 000)	(>18 000)	(>25 000)	(>392)
19		12.34[b]	0.015[b]	0.007[b]		0.017
(SI,[a] VERO)			(823)	(1763)		(726)

[a] SI = PBMC (VERO)/biological activity. [b] Results taken from ref 5.

Additional information about the activity of our tetraoxanes was obtained from cytotoxicity screening against normal human peripheral blood mononuclear cells (PBMC). The IC_{50} values for compound **13** in both tests, using nonstimulated and phytohemaglutinine (PHA)-stimulated PBMC,[3a] were >200 μM indicating very low toxicity of the tested compound on healthy cells. The high selectivity values (Table 5) combined with pronounced antimalarial and high antiproliferative activity of **13**, in addition to extremely high antiproliferative activity of **19** (with maximum tolerated dose (MTD) determined at NCI, 400 mg/kg) indicate that tetraoxanes should be more closely scrutinized as possible anticancer drug leads, as well.

Having in mind the relative metabolic stability of tested tetraoxanes (no peroxide bond scission observed in in vitro ADME studies), it is very likely that tetraoxanes undergo the peroxide cleavage within the parasite or infected RBCs to yield RO• radicals together with toxic Fe(IV)═O species,[36,37] both of which are capable of inducing lethal lipid peroxidation.

Tetraoxanes are stable in the parasite food vacuole's pH 5.0−5.4 (tetraoxane **15** was found to be stable within pH range 1.6−12); however, the possibility of a "retro-peroxyacetalization" reaction or a C-centered radical generation in situ (RBC membrane, parasite's membrane, cytosol, or FV) cannot be presently excluded, specifically in view of Wu's experiments.

To conclude, by this work we have confirmed that the examined tetraoxanes are potent, nontoxic antimalarials and antiproliferatives. In addition, the results of our experiments for the first time bring to light the existence of RO• radicals (derived from a peroxide with antimalarial activity) that may play an important role inducing the "killing event" in plasmodium species or, even, of the cancer cell.

Experimental Procedures

General. Melting points were determined on a Boetius PMHK apparatus and were not corrected. Optical rotation measurements were performed on a Perkin-Elmer 341 polarimeter at the given temperatures. Concentrations are expressed in grams per 100 mL. IR spectra were recorded on a Perkin-Elmer spectrophotometer FT-IR 1725X. ^1H and ^{13}C NMR spectra were recorded on a Varian Gemini-200 spectrometer (at 200 and 50 MHz, respectively) in the indicated solvent using TMS as internal standard. Chemical shifts are expressed in ppm (δ) values and coupling constants (J) in Hz. ESI mass spectra of synthesized compounds were acquired on a TSQ (Thermo Quest; Finnigan) triple quadrupole instrument. Samples were dissolved in pure acetonitrile (HPLC grade). For positive ions conditions were as follows: capillary temperature 250 °C; ESI spray voltage 4.5 kV; multiplier 1500 V; loop injection

into a solution of $H_2O/CH_3CN/HCOOH$ (1%) = 18:80:2 (v/v/v); flow rate 0.3 mL/min. For negative ions conditions were as follows: capillary temperature 250 °C; ESI spray voltage 4.5 kV; multiplier 1500 V; loop injection into a solution of $H_2O/CH_3CN/HCOOH$ (1%)/$CH_3CO_2NH_4$ (10 mmol) 9:80:1:10 (v/v/v/v); flow rate 0.3 mL/min. MS-CI spectra were recorded on a MS Finnigan-MAT 8230 spectrometer with double focusing reverse geometry, using isobutane. Lobar LichroPrep Si 60 (40−63 μm) or LichroPrep RP-18 columns coupled to a Waters RI 401 detector were used for column chromatography. Where appropriate, the compounds are listed according to their elution order.

For metabolism experiments, incubations were separated on a Waters XTerra 3.5 μm, 2.0 mm × 50 mm C18 column using a formic acid/acetonitrile mobile phase. They were analyzed using a Surveyor separations module coupled to a ThermoFinnigan TSQ AM triple quadrupole mass spectrometer. Mass spectral analyses were done using electrospray ionization in positive ion mode.

gem-Dihydroperoxyde **2** and tetraoxanes **4** were synthesized according to procedures described previously.[5]

Methyl 7α,12α-Diacetoxy-5β-cholan-24-oate-3-spiro-6′-(1′,2′,4′,5′-tetraoxacyclohexane)-3′-spiro-1″-((4″*R*)- and (4″*S*)-methoxycarbonyl)cyclohexanes (4). To the cold solution (ice-bath) of dihydroperoxide **2** (5.15 g, 9.3 mmol) in CH_2Cl_2 (130 mL), ketone **3** (18.6 mmol) was added, and after 30 min of stirring at same temperature, 5 × 650 μL of ice-bath cooled H_2SO_4/CH_3CN mixture (1:10, v/v) was added dropwise in 15 min intervals. After an additional 15 min of stirring, the reaction mixture was worked-up in a usual manner and was purified by column chromatography (dry-flash SiO_2, eluent heptane/EtOAc = 8/2 followed by Lobar B, LichroPrep RP-18, eluent MeOH/H_2O = 8/2) affording 1.74 g (27%) of tetraoxane **4** as mixture of epimers.

Propyl 7α,12α-Diacetoxy-5β-cholan-24-oate-3-spiro-6′-(1′,2′,4′,5′-tetraoxacyclohexane)-3′-spiro-1″-((4″*R*)- and (4″*S*)-propoxycarbonyl)cyclohexane (5a and 5b). The mixture of epimers **4** (2 g) was transformed into corresponding propyl esters **5a** and **5b** using anh. K_2CO_3 (1.6 g, 11.6 mmol) in dry *n*-PrOH (80 mL) at 80 °C. After 2 h, the reaction was cooled and diluted with 40 mL of H_2O and 100 mL of CH_2Cl_2. The water layer was acidified to pH 2 with diluted HCl, the layers were separated, and the water layer was extracted with CH_2Cl_2 (3 × 30 mL). Combined organic layers were washed with water and brine, dried over anh. Na_2SO_4, evaporated to dryness, and purified by column chromatography (Lobar B, LichroPrep Si 60, eluent heptane/EtOAc = 85/15).

5a (4″*R*): Yield 577 mg, colorless foam softness at 58−60 °C. $[\alpha]_D^{20} = +31.5$ ($c = 0.054$, $CHCl_3$). Anal. ($C_{41}H_{64}O_{12}\cdot 0.5H_2O$) C, H.

5b (4″*S*): Yield 509 mg, colorless foam softness at 155−160 °C. $[\alpha]_D^{20} = +50.0$ ($c = 0.060$, $CHCl_3$). Anal. ($C_{41}H_{64}O_{12}\cdot 0.5H_2O$) C, H.

7α,12α-Diacetoxy-5β-cholan-24-oic Acid 3-Spiro-6′-(1′,2′,4′,5′-tetraoxacyclohexane)-3′-spiro-1″-((4″*R*)-carboxy)cyclohexane (6a). Propyl ester **5a** (308 mg, 0.41 mmol) was hydrolyzed at 80 °C with NaOH (50 mg, 1.25 mmol) in an *i*-PrOH/H_2O mixture (16 mL, 3:1 v/v). After 15 min, the reaction was cooled and diluted with 20 mL of H_2O and 50 mL of CH_2Cl_2. The water layer was acidified to pH 2 with diluted HCl, and the layers were separated. The water layer was further extracted with CH_2Cl_2 (3 × 30 mL); combined organic layers were washed with water and brine, dried over anh. Na_2SO_4, and evaporated to dryness. Yield 265 mg (97%); mp = 150−155 °C (EtOAc/heptane). $[\alpha]_D^{20} = +50.0$ ($c = 0.052$, $CHCl_3$). Anal.($C_{35}H_{52}O_{12}\cdot 0.5H_2O$) C, H.

7α,12α-Diacetoxy-5β-cholan-24-oic Acid 3-Spiro-6′-(1′,2′,4′,5′-tetraoxacyclohexane)-3′-spiro-1″-((4″*S*)-carboxy)cyclohexane (6b). Propyl ester **5b** (555 mg, 0.74 mmol) was hydrolyzed to acid **6b** using the same procedure as that given for **6a**. Yield 484 mg (98%); mp = 155−158 °C (EtOAc/heptane). $[\alpha]_D^{20} = +56.8$ ($c = 0.074$, $CHCl_3$). Anal.($C_{35}H_{52}O_{12}\cdot H_2O$) C, H.

General Procedure for Preparation of Amides 7−14. A solution of **6a** (113 mg, 0.17 mmol) in dry CH_2Cl_2 (10 mL) with added Et_3N (47.8 μL, 0.34 mmol) and $ClCO_2Et$ (32 μL, 0.34 mmol) was stirred for 60 min at 0 °C. A given amount of amine was added, and after 30 min of stirring, the reaction mixture was warmed to rt. After 90 min, it was diluted with H_2O, the layers were separated, and the organic layer was washed with brine, dried over anh. Na_2SO_4, and evaporated to dryness. The crude product was purified by dry-flash chromatography.

7α,12α-Diacetoxy-5β-cholan-24-amide-3-spiro-6′-(1′,2′,4′,5′-tetraoxacyclohexane)-3′-spiro-1″-((4″*R*)-carbamoyl)cyclohexane (7). Employing the above given procedure, compound **6a** reacted with 20 equiv of NH_4Cl and 20 equiv of Et_3N in dry CH_2Cl_2 (20 mL) to afford the primary amide **7** (97 mg, 87%). The crude product was purified using dry-flash chromatography, eluent EtOAc/MeOH/NH_3 (8/1/1). Colorless foam softness at 158−162 °C. $[\alpha]_D^{20} = +51.5$ ($c = 0.068$, $CHCl_3$). Anal. ($C_{35}H_{54}N_2O_{10}\cdot H_2O$) C, H, N.

7α,12α-Diacetoxy-5β-cholan-24-amide-3-spiro-6′-(1′,2′,4′,5′-tetraoxacyclohexane)-3′-spiro-1″-((4″*S*)-carbamoyl)cyclohexane (8). Acid **6b** (100 mg, 0.15 mmol) was transformed into amide **8** (84 mg, 85%) using a suspension of 20 equiv of NH_4Cl and 20 equiv of Et_3N in dry CH_2Cl_2 (20 mL). The crude product was purified using dry-flash chromatography, eluent EtOAc/MeOH/NH_3 (8/1/1). Crystallization from EtOAc/heptane afforded colorless crystals, mp = 165−167 °C. $[\alpha]_D^{20} = +55.6$ ($c = 0.072$, $CHCl_3$). Anal. ($C_{35}H_{54}N_2O_{10}\cdot H_2O$) C, H, N.

X-ray Analysis of 8. The X-ray intensity data were collected at 100 K with a MAR345 image plate using Mo Kα ($\lambda = 0.710\,69$ Å) radiation. A crystal of approximate dimensions 0.32 × 0.30 × 0.12 mm^3 was chosen, mounted in inert oil, and transferred to the cold gas stream for flash cooling. The unit cell parameters were refined using all the collected spots after the integration process. Molecular formula = $C_{163}H_{258}N_8O_{52}$, $M_r = 3161.8$, monoclinic, *C*2, $a = 44.540(12)$, $b = 16.362(5)$, $c = 29.574(9)$ Å, $\beta = 99.42(3)°$, $V = 21262(11)$ $Å^3$, $Z = 4$, $D_x = 0.99$ g·cm^{-3}, $\mu = 0.073$ mm^{-1}, $F(000) = 6832$, $T = 100$ K.

A total of 38 085 reflections were collected from 95 images taken at a crystal to detector distance of 170 mm. There are 23 601 independent refections ($R_{int} = 0.051$). The structure was solved by direct methods using SHELXS97[38] and refined by full-matrix block least-squares on F^2 using SHELXL97.[38] All the non-hydrogen atoms of the four tetraoxanes, the heptane, and the ethyl acetate molecules were refined anisotropically. The hydrogen atoms were calculated with AFIX and included in the refinement with a common isotropic temperature factor. The H atoms of the NH_2, of the four water molecules, of the acetone, and of the methanol solvent molecules were not localized. Final *R* values are $R = 0.096$ for 20 973 observed reflections, *R*(all data) = 0.105, $wR = 0.265$, and $S = 1.05$. The data have been deposited with the Cambridge Crystallographic Data Centre (No. CCDC 284790).

***N*-Propyl-7α,12α-diacetoxy-5β-cholan-24-amide-3-spiro-6′-(1′,2′,4′,5′-tetraoxacyclohexane)-3′-spiro-1″-((4″*R*)-propylcarbamoyl)cyclohexane (9).** Acid **6a** (113 mg, 0.17 mmol) was transformed into amide **9** (106 mg, 84%) using 10 equiv of *n*-$PrNH_2$ in dry CH_2Cl_2 (20 mL). The crude product was purified using dry-flash chromatography, EtOAc/heptane = 7/3. Colorless foam softness at 128−132 °C. $[\alpha]_D^{20} = +45.5$ ($c = 0.066$, $CHCl_3$). Anal. ($C_{41}H_{66}N_2O_{10}\cdot 1.5H_2O$) C, H, N.

***N*-Propyl-7α,12α-diacetoxy-5β-cholan-24-amide-3-spiro-6′-(1′,2′,4′,5′-tetraoxacyclohexane)-3′-spiro-1″-((4″*S*)-propylcarbamoyl)cyclohexane (10).** Acid **6b** (100 mg, 0.15 mmol) was transformed into amide **10** (95 mg, 85%) using 10 equiv of *n*-$PrNH_2$ in dry CH_2Cl_2 (20 mL). The crude product was purified using dry-flash chromatography, EtOAc/heptane = 7/3. Colorless foam softness at 126−128 °C. $[\alpha]_D^{20} = +53.1$ ($c = 0.064$, $CHCl_3$). Anal. ($C_{41}H_{66}N_2O_{10}\cdot 2.5H_2O$) C, H, N.

***N*-(2-Dimethylamino)ethyl-7α,12α-diacetoxy-5β-cholan-24-amide-3-spiro-6′-(1′,2′,4′,5′-tetraoxacyclohexane)-3′-spiro-1″-((4″*R*)-(2-dimethylamino)ethylcarbamoyl)cyclohexane (11).** Acid **6a** (113 mg, 0.17 mmol) was transformed into amide **11** (124 mg, 91%) using 10 equiv of $Me_2NCH_2CH_2NH_2$ in dry CH_2Cl_2 (20 mL). The crude product was purified using dry-flash chromatography,

EtOAc/MeOH/NH_3 = 8/1/1. Colorless foam softness at 65−68 °C. $[\alpha]_D^{20}$ = +40.8 (*c* = 0.076, $CHCl_3$). Anal. ($C_{43}H_{72}N_4O_{10}\cdot H_2O$) C, H, N.

***N*-(2-Dimethylamino)ethyl-7α,12α-diacetoxy-5*β*-cholan-24-amide-3-spiro-6′-(1′,2′,4′,5′-tetraoxacyclohexane)-3′-spiro-1″-((4″*S*)-(2-dimethylamino)ethylcarbamoyl)cyclohexane (12).** Acid **6b** (100 mg, 0.15 mmol) was transformed into amide **12** (108 mg, 89%) using 10 equiv of $Me_2NCH_2CH_2NH_2$ in dry CH_2Cl_2 (20 mL). The crude product was purified using dry-flash chromatography, EtOAc/MeOH/NH_3 = 8/1/1. Colorless foam softness at 110−114 °C. $[\alpha]_D^{20}$ = +48.1 (*c* = 0.052, $CHCl_3$). Anal. ($C_{43}H_{72}N_4O_{10}\cdot H_2O$) C, H, N.

***N*-Phenyl-7α,12α-diacetoxy-5*β*-cholan-24-amide-3-spiro-6′-(1′,2′,4′,5′-tetraoxacyclohexane)-3′-spiro-1″-((4″*R*)-phenylcarbamoyl)cyclohexane (13).** Acid **6a** (113 mg, 0.17 mmol) was transformed into amide **13** (116 mg, 84%) using 10 equiv of $PhNH_2$ in dry CH_2Cl_2 (20 mL). The crude product was purified using dry-flash chromatography, heptane/EtOAc = 6/4. Colorless foam softness at 157−162 °C. $[\alpha]_D^{20}$ = +34.0 (*c* = 0.05, $CHCl_3$). Anal. ($C_{47}H_{62}N_2O_{10}\cdot 4H_2O$) C, H, N.

***N*-Phenyl-7α,12α-diacetoxy-5*β*-cholan-24-amide-3-spiro-6′-(1′,2′,4′,5′-tetraoxacyclohexane)-3′-spiro-1″-((4″*S*)-phenylcarbamoyl)cyclohexane (14).** Acid **6b** (100 mg, 0.15 mmol) was transformed into amide **14** (106 mg, 87%) using 10 equiv of $PhNH_2$ in dry CH_2Cl_2 (20 mL). The crude product was purified using dry-flash chromatography, heptane/EtOAc = 6/4. Colorless foam softness at 161−165 °C. $[\alpha]_D^{20}$ = +51.9 (*c* = 0.052, $CHCl_3$). Anal. ($C_{47}H_{62}N_2O_{10}\cdot H_2O$) C, H, N.

Bis(*N*-(phenyl)-3-dioxy-7α,12α-diacetoxy-5*β*-cholan-24-amide) (21). Bis-steroidal acid (compound **15** in ref 3a, 119.1 mg, 0.12 mmol) was transformed into amide **21** (102.0 mg, 75%) according to the general procedure using 4 equiv of $PhNH_2$ (43 μL, 0.47 mmol) and purified by column chromatography, Lobar B, LichroPrep Si 60, eluent EtOAc/heptane = 1/1. Colorless foam, softness at 188−190 °C. $[\alpha]_D^{20}$ = +31.53 (c = 1.1, $CHCl_3$). Anal. ($C_{68}H_{94}N_2O_{14}\cdot H_2O$): C, H, N.

In Vitro Antimalarial Activity. The in vitro antimalarial drug susceptibility screen is a modification of the procedures first published by Desjardins et al.,[39] with modifications developed by Milhous et al.,[40] and the details are given in ref 3a. Two *P. falciparum* clones, D6 and W2, and one multidrug-resistant isolate from Thailand, TM91C235, were used for the in vitro screening of 12 synthesized mixed tetraoxanes. W2 is resistant to chloroquine, quinine, and pyrimethamine and susceptible to mefloquine. D6 tends to be more resistant to mefloquine and susceptible to chloroquine, quinine, and pyrimethamine.

In Vivo Antimalarial Activity. The *P. berghei* mouse efficacy tests were conducted at the University of Miami using a modified version of the Thompson test. Basically, groups of five mice were inoculated intraperitoneally with erythrocytes infected with a drug-sensitive strain of *P. berghei* on day 0. Drugs were suspended in 0.5% hydroxyethylcellulose−0.1% Tween 80 and administered orally beginning on day 3 post infection. Dosing was at 50, 200, and 600 $mg\cdot kg^{-1}\cdot day^{-1}$ for 3 days. Cure was defined as survival until day 31 posttreatment. Untreated control mice usually die on day 6−10 postinfection.

Metabolic Stability Analysis and Metabolite Determination. The metabolic stability assay sample preparation was performed in a 96-well plate on a TECAN Genesis robotic sample processor following WRAIR SOP SP 01-02. All incubations were carried out in 0.1 M sodium phosphate buffer (pH 7.4) in the presence of an NADPH-regenerating system (NADP+ sodium salt, $MgCl_2\cdot 6H_2O$, and glucose-6-phosphate). Test drug (10 μM), microsomes (1 mg/mL total protein), buffer, and NADPH-regenerating system were warmed to 37 °C, and the reaction was initiated by the addition of glucose-6-phosphate dehydrogenase (G6PD). Samples were quenched at 0, 10, 30, and 60 min using an equal volume of cold methanol. Samples were centrifuged to pellet the proteins, and the supernatant was analyzed by LC-MS/MS using fast LC gradient or isocratic methods. Parent drug was quantified using external calibration, using plots of parent drug response vs. amount. Chromatograms were analyzed using the mass spectrometry software Xcalibur QuanBrowser. Concentrations of parent drug remaining at each time point were calculated using the unknown peak areas and corresponding calibration curves. To calculate the half-life, a first-order rate of decay was assumed. A plot of the natural log(LN) of the drug concentration versus time was generated, where the slope of that line was $-k$. Half-life was calculated as 0.693/*k*. Hepatic microsomal intrinsic clearance was calculated using the formula $CL_{int,in\ vitro}$ = (rate/min) × (mL/0.5 g) × 52.5 mg/g liver or $CL_{int,in\ vitro} = k \times$ (microsomal protein content per gram of liver)/(microsomal protein concentration in incubation buffer).

For metabolite identification, samples were prepared as described above with human liver microsomes. Additional samples were prepared with each drug using mouse, rat, and rhesus monkey liver microsomes. Samples were separated using an LC gradient or isocratic method and analyzed by full scan LC-MS and LC-MS/MS. Parent compound and putative metabolites were all fragmented, and these MS/MS experiments were used in combination with the no-NADPH control experiments to confirm the assignment of peaks as metabolites. These MS/MS data were also used to do preliminary structural elucidation of metabolites of **7**. ESI-MS/MS (**7**): *m*/*z* 663 $[M + H]^+$ (10), *m*/*z* 603 $[MH - OAc]^+$ (83), *m*/*z* 543 $[MH - 2OAc]^+$ (100), *m*/*z* 522 (61), *m*/*z* 462 (44), *m*/*z* 420 (41). LC-MS/MS of the hydroxylated metabolite ($[MH + 16]^+$) of **7**: *m*/*z* 679 $[M + H]^+$ (36), *m*/*z* 619 $[MH - OAc]^+$ (100), *m*/*z* 559 $[MH - 2OAc]^+$ (24), *m*/*z* 538 (54), *m*/*z* 478 (41), *m*/*z* 418 (42). LC-MS/MS of the dihydroxylated metabolite ($[MH + 32]^+$) of **7**: *m*/*z* 695 $[M + H]^+$ (11), *m*/*z* 635 $[MH - OAc]^+$ (100), *m*/*z* 575 $[MH - 2OAc]^+$(14), *m*/*z* 478 (4), *m*/*z* 368 (6).

Preliminary Stability Study. Stability tests revealed that exemplary compound **15** is stable at pH 1.60, 5, and 12: (1) pH 1.6, CH_3OH (6.7 mL), HCl (0.10448 M, 3.30 mL), **15** (7.0 mg) was dissolved in the buffered solution (10.0 mL) and was kept at 37 °C for 4 days; (2) pH 5.0, oxalic acid in CH_3OH (0.02 M 85.5 mL) + $LiOCH_3$ in CH_3OH (0.02 M, 14.5 mL), **15** (30 mg) was dissolved in the buffered solution (5.0 mL) and was kept at rt for 4 days; (3) pH 12, NaOH (50 mg), i-PrOH/H_2O (16 mL, 3:1, v/v), conditions used for ester hydrolysis to obtain acid (**5a** → **6a**), rt → 80 °C, tested up to 2 days.

Reaction with Fe(II). Isolation of products. 3-Oxo-7α,12α-diacetoxy-5*β*-cholan-24-amide (26) from 20. Bis-tetraoxane **20** (68.3 mg, 0.068 mmol) was treated with $FeCl_2\cdot 4H_2O$ (26.8 mg, 0.135 mmol) in acetonitrile (5 mL) at rt for 5 h. The iron species were precipitated upon centrifugation, the solution was evaporated, and the crude product was purified through a SiO_2 column (Lobar A, LichroPrep Si-60, eluent EtOAc). Ketone **26** (identical with the one prepared earlier)[3a] was isolated in 97% yield (64.1 mg). When the reaction was repeated twice, ketone **26** was isolated in 95% and 95.5% yield.

***N*-(Phenyl)-3-oxo-7α,12α-diacetoxy-5*β*-cholan-24-amide (27) from 21.** Likewise, tetraoxane **21** (102.0 mg, 0.088 mmol) was treated with $FeCl_2\cdot 4H_2O$ (34.7 mg, 0.175 mmol) in acetonitrile (10 mL). The iron species were precipitated upon centrifugation, the solution was evaporated, and the crude product was purified through a SiO_2 column (Lobar A, LichroPrep Si-60, eluent EtOAc/heptane = 4/6). Ketone **27** was isolated in 95% yield (94.3 mg) as colorless foam, mp 214−216 °C. $[\alpha]_D^{20}$ = + 51.0 (*c* = 1.05, CH_2CH_2). Anal. ($C_{34}H_{47}NO_6\cdot 2.5\ H_2O$): C, H, N.

Ketone 27 and 4-oxo-*N*-phenylcyclohexanecarboxamide (28) from 13. Tetraoxane **13** (15.0 mg, 0.01 mmol) was treated with $FeCl_2\cdot 4H_2O$ (39.8 mg, 0.02 mmol) in acetonitrile (10 mL). The iron species were precipitated upon centrifugation, the solution was evaporated, and the crude product was analyzed by HPLC using LiChrospher 100 RP-18 (5 μm, 250 mm × 4 mm) column (eluent 0.1% H_3PO_4/acetonitrile, gradient, flow 1 mL/min, 25 °C). The obtained chromatogram revealed the existence of only two products with retention times of 4.53 min (**28**) and 12.52 min (**22**) in the ratio of ca. 1.05:1. Purification of crude mixture using SiO_2 column (Lobar A, LichroPrep Si-60, eluent EtOAc/heptane = 4/6) afforded ketones **27** and **28** in 84% (47.1 mg) and 96% (20.7 mg) yield,

respectively. Spectral and analytical data for ketone **27** isolated were identical to the ones above. Ketone **28**: colorless foam softness at 165−168 °C. Anal. ($C_{13}H_{15}NO_2$) C, H, N.

EPR Spectroscopy. The EPR spectra with DMPO as a spin trap were recorded on a Varian E-109 apparatus. The EPR instrumental settings for experiments were the following: H = 3187 G (center field), microwave frequency = 8.98 GHz, modulation frequency = 100 kHz, field sweep = 200 G, modulation amplitude = 2.5 G, receiver gain 2.5×10^3, microwave power = 15 mW, time constant = 128 ms, sweep time = 4 min. Program for the simulation of EPR spectra and the spin trap database are readily available to the public through the Internet (http://EPR.niehs.nih.gov/).

The EPR spectra with DEPMPO as a spin trapper were recorded on a Varian E-104-A. The EPR instrumental settings for experiment were the following: H = 3410 G (center field), microwave frequency = 9.51 GHz, modulation frequency = 100 kHz, field sweep = 200 G, modulation amplitude = 2 G, receiver gain 2×10^4, microwave power = 10 mW, time constant = 32 ms, sweep time = 2 min. WINEPR SimFonia, v1.25, was used for the simulation of DEPMPO generated EPR spectra.

Typical procedure was as follows: $FeCl_2 \cdot 4H_2O$ (2.0 mM, final concentration upon mixing), tetraoxane (2.0 mM), DMPO (200 mM, final concentration upon mixing) or DEPMPO (112.5 mM, final concentration upon mixing), oxygen-free acetonitrile, room temperature. Strong EPR signals were observed within 5−6 min.

EPR spectra of DMPO-•OR and DEPMPO-•OR radicals obtained by carrying Fe(II)-induced reductive scission of mixed tetraoxanes **23**, **24**, and **25** are given as Supporting Information.

Fe(IV)=O Species.[29] $FeCl_2 \cdot 4H_2O$ (11 mg, 0.055 mmol) and CH_3CN (2 mL) were placed in a dried flask under argon. The mixture was cooled to 0 °C, followed by the addition of HMDB (55.8 μL, 0.277 mmol) and tetraoxane **25** (15.8 mg, 0.055 mmol) to the reaction. The reaction mixture was stirred at 0 °C for 60 min and quenched with water, and water layer was extracted with (a) pentane, (b) pentane−Et_2O, and (c) Et_2O. GC-MS analysis revealed that extract a consists of HMDB and HMB and extracts b and c consist of two product ketones, cyclohexanone and methyl 4-oxocyclohexanecarboxylate, HMDB, and HMB. GC conditions were as follows: Finnigan ion trap detector ITD-705 was used with Varian 3400 GC equipped with SGE OCI-5 cold on column injector; column Supelco PTE-5 30 m, 0.32 mm id, 0.25 μm film, inserted directly in the ion trap via the transfer line at 240 °C; carrier gas hydrogen, 0.5 mL/min; ion manifold and exit nozzle temperatures of 240 °C were used; column temperature was linearly programmed from 40 to 285 °C at 4.3 °C/min; scan range was 39−333 Da, l scan/s (five micro scans were averaged); tuning parameters were 10, 50, 50, 100; B 9000; AGC on, background mass 33; version 3 of ITDS software was used. The second system was a Varian 3400 GC equipped with a split/splitless injector (1: 99) operated at 266 °C, column J&W Scientific DB-5ms-ITD 30 m, 0.25 mm id, 0.25 μm film, carrier gas hydrogen, l mL/min measured at 210 °C; column temperature was linearly programmed from 40 to 285 °C at 4.3°/min; transfer line at 270 °C, coupled to Finnigan-MAT 8230 BE mass spectrometer; ion source temperature 170 °C, EI, 70 eV 0.1 mA. Library search and mass spectral deconvolution and extraction were performed using AMDIS (Automated Mass Spectral Deconvolution and Identification System) software, version 2.0β or v2.1 and v2.61, using RI calibration data analysis parameters calibrated with a series of *n*-alcanes. Search was performed against our compilation of spectra.

In case of ITD spectra taken under the above-reported conditions, *m*/*z* 77 ("Black Hole") was suppressed. The NIST 2k library was used for the main search.

Acknowledgment. This work has been supported by the Ministry of Science and Environmental Protection of Serbia (Grant No. 142022). The DAAD stipend to N.T. is greatly acknowledged. The authors from Belgrade are indebted to Sylvia Marzian from University of Dortmund for running the ESI-MS spectra. We thank the NIH-NCI's Developmental and Therapeutics program for evaluation of our tetraoxanes. Material has been reviewed by the Walter Reed Army Institute of Research. There is no objection to its presentation or publication. The opinions or assertions contained herein are the private views of the author and are not to be construed as official or as reflecting true views of the Department of the Army or the Department of Defense.

Supporting Information Available: Spectroscopic data of synthesized and isolated compounds, EPR spectra of Fe(II)-induced reactions of geminal dihydroperoxide **2**, and mixed tetraoxanes **23**, **24**, and **25**, together with EPR of tetraoxane **23** monitored for 22 h using DMPO or DEPMPO as radical trappers, and elemental analysis of the compounds. This material is free of charge via the Internet at http://pubs.acs.org.

References

(1) Malaria Foundation International, http://www.malaria.org/, and the sites given therein.

(2) (a) Vennerstrom, J. L.; Fu, H.-N.; Ellis, W. Y.; Ager, A. L, Jr.; Wood, J. K.; Andersen, S. L.; Gerena, L.; Milhous, W. K. Dispiro-1,2,4,5-tetraoxanes: a new class of antimalarial peroxides. *J. Med. Chem.* **1992**, *35*, 3023−3027. (b) Todorović, N. M.; Stefanović, Tinant, M. B.; Declercq, J.-P.; Makler, M. T.; Šolaja, B. A. Steroidal Geminal Dihydroperoxides and 1,2,4,5-tetraoxanes: Structure Determination and their Antimalarial Activity. *Steroids* **1996**, *61*, 688−696.

(3) (a) Opsenica, D.; Pocsfalvi, G.; Juranić, Z.; Tinant, B.; Declercq, J.-P.; Kyle, D. E.; Milhous, W. K.; Šolaja, B. A. Cholic Acid Derivatives as 1,2,4,5-Tetraoxane Carriers: Structure and Antimalarial and Antiproliferative Activity. *J. Med. Chem.* **2000**, *43*, 3274−3282. (b) Opsenica, D.; Angelovski, G.; Pocsfalvi, G.; Juranić, Z.; Žižak, Z.; Kyle, D.; Milhous, W. K.; Šolaja, B. A. Antimalarial and Antiproliferative Evaluation of Bis-Steroidal Tetraoxanes. *Bioorg. Med. Chem.* **2003**, *11*, 2761−2768.

(4) (a) Vennerstrom, J. L.; Dong, Y. S.; Andersen, L.; Ager, A. L., Jr.; Fu, H.-N.; Miller, R. E.; Wesche, D. L.; Kyle, D. E.; Gerena, L.; Walters, S. M.; Wood, J. K.; Edwards, G.; Holme, A. D.; McLean, W. G.; Milhous, W. K. Synthesis and Antimalarial Activity of Sixteen Dispiro-1,2,4,5-tetraoxanes: Alkyl-Substituted 7,8,15,16-Tetraoxadispiro[5.2.5.2]hexadecanes. *J. Med. Chem.* **2000**, *43*, 2753−2758 and references therein. (b) Vennerstrom, J. L.; Ager, A. L.; Andersen, S. L.; Grace, J. M.; Wongpanich, V. C.; Angerhofer, K.; Hu, J. K.; Wesche, D. L. Assessment of the Antimalarial Potential of Tetraoxane WR148999. *Am. J. Trop. Med. Hyg.* **2000**, *62*, 573−578.

(5) Šolaja, B. A.; Terzić, N.; Pocsfalvi, G.; Gerena, L.; Tinant, B.; Opsenica, D.; Milhous, W. K. Mixed Steroidal 1,2,4,5-Tetraoxanes: Antimalarial and Antimycobacterial Activity. *J. Med. Chem.* **2002**, *45*, 3331−3336.

(6) (a) Kim, H.-S.; Tsuchiya, K.; Shibata, Y.; Wataya, Y.; Ushigoe, Y.; Masuyama, A.; Nojima, M.; McCullough, K. J. Synthetic Methods for Unsymmetrically substituted 1,2,4,5-tetroxanes and of 1,2,4,5,7-pentoxocanes. *J. Chem. Soc., Perkin Trans 1* **1999**, 1867−1870. (b) Iskra, J.; Bonnet-Delponb, D.; Bégue, J.-P. One-pot synthesis of nonsymmetric tetraoxanes with the H_2O_2/MTO/fluorous alcohol system. *Tetrahedron Lett.* **2003**, *44*, 6309−6312.

(7) Opsenica, D.; Kyle, E.; Milhous, W. K.; Šolaja, B. A. Antimalarial, antimycobacterial and antiproliferative activity of phenyl substituted mixed tetraoxanes. *J. Serb. Chem. Soc.* **2003**, *68*, 291−302.

(8) O'Neill, P. M.; Posner, G. H. A Medicinal Chemistry Perspective on Artemisinin and Related Endoperoxides. *J. Med. Chem.* **2004**, *47*, 2945−2964 and references therein.

(9) Eckstein-Ludwig, U.; Webb, R. J.; van Goethem, I. D. A.; East, J. M.; Lee, A. G.; Kimura, M.; O'Neill, P. M.; Bray, P. G.; Ward, S. A.; Krishna, S. Artemisinins Target the Serca of *Plasmodium falciparum*. *Nature* **2003**, *424*, 957−961.

(10) Robert, A.; Dechy-Cabaret, O.; Cazelles, J, Meinier, B. From Mechanistic Studies on Artemisinin Derivatives to New Modular Antimalarial Drugs. *Acc. Chem. Res.* **2002**, *35*, 167−174.

(11) Berman, P. A.; Adams, P. A. Artemisinin Enhances Heme-Catalysed Oxidation of Lipid Membranes. *Free Radical Biol. Med.* **1997**, *22*, 1283−1288.

(12) IC_{90} can be envisaged to represent a suitable compromise between the substantial amount of data obtainable with IC_{50} (value based on a relatively high number of parasites, but with less relevance to the therapeutic situation) and IC_{99} (reflects MIC and full efficacy, however, based on a relatively small number of surviving parasites available for analysis).

(13) Vennerstrom, J. L.; Arbe-Barnes, S.; Brun, R.; Charman, S. A.; Chiu, F. C. K.; Chollet, J.; Dong, Y.; Dorn, A.; Hunziker, D.; Matile, H.; McIntosh, K.; Padmanilayam, M.; Santo Tomas, J.; Scheurer, C.; Scorneaux, B.; Tang, Y.; Urwyler, H.; Wittlin, S.; Charman, W. N. Identification of an antimalarial synthetic trioxolane drug development candidate. *Nature* **2004**, *430*, 900−904.

(14) (a) Posner, G. H.; McRiner, A. J.; Paik, I. H.; Sur, S.; Borstnik, K.; Xie, S.; Shapiro, T. A.; Alagbala, A.; Foster, B. Anticancer and Antimalarial Efficacy of Artemisinin-Derived trioxane Dimers in Rodents. *J. Med. Chem.* **2004**, *47*, 1299−1301. (b) Paik, I. H.; Xie, S.; Shapiro, T. A.; Tanzina Labonte, T.; Narducci Sarjeant, A. A.; Baege, A. C.; Posner, G. H. Second Generation, Orally Active, Antimalarial, Artemisinin-Derived Trioxane Dimers with High Stability, Efficacy, and Anticancer Activity. *J. Med. Chem.* **2006**, *49*, 2731−2734.

(15) Drug discovery and development program, National Cancer Institute, Bethesda, MD (NCI), http://dtp.nci.nih.gov.

(16) Tang, Y., Dong, Y., Wang, X., Sriraghavan, K., Wood, J. K., Vennerstrom, J. L. Dispiro-1,2,4-trioxane Analogues of a Prototype Dispiro-1,2,4-troxolane: Mechanistic Comparators for Artemisinin in the Context of reaction pathways with Iron (II). *J. Org. Chem.* **2005**, *70*, 5103−5110.

(17) Tonmunphean, S.; Wijitkosoom, A.; Tantirungrotechai, Y. Influence of Stereoisomer of dispiro-1,2,4,5-tetraoxanes on their binding mode with heme and on antimalarial activity: molecular docking studies. *Bioorg. Med. Chem.* **2004**, *12*, 2005−2012.

(18) Liu, H.-H.; Wu, Y.-K.; Shen, X. Alkylation of Sulfur Ligand in Cysteinate-Iron Chelates by a 1,2,4,5-Tetraoxane. *Chin. J. Chem.* **2003**, *21*, 875−877.

(19) Jefford, C. W.; Vicente, M. G. H.; Jacquier, Y.; Favarger, F.; Mareda, J.; Millasson Schmidt, P.; Brunner, G.; Burger, U. The Deoxygenation and Isomerization of Artemisinin and Artemether and their Relevance to Antimalarial Action. *Helv. Chim. Acta* **1996**, *79*, 1475−1487.

(20) O'Neill, P. M.; Miller, A.; Bishop, L. P. D.; Hindley, S.; Maggs, J. L.; Ward, S. A.; Roberts, S. M.; Scheinmann, F.; Stachulski, A. V.; Posner, G. H.; Park, B. K. Synthesis, Antimalarial Activity, Biomimetic Iron(II) Chemistry, and in Vivo Metabolism of Novel, Potent *C*-10-Phenoxy Derivatives of Dihydroartemisinin. *J. Med. Chem.* **2001**, *44*, 58−68.

(21) For preparation of bis-steroidal tetraoxanes, see ref 3a.

(22) With less than 2 equiv of $FeCl_2 \cdot 4H_2O$, the reaction did not go to completion.

(23) Compound **24** was synthesized using conditions given in ref 5. Full analytical details and biological data will be published shortly elsewhere.

(24) Opsenica, I.; Terzić, N.; Opsenica, D.; Milhous, W. K.; Šolaja, B. 7,8,15,16-Tetraoxa dispiro[5.2.5.2]hexadecane-3-carboxylic Acid Derivatives and Their Antimalarial Activity. *J. Serb. Chem. Soc.* **2004**, *69*, 919−922.

(25) Jones, C. M.; Burkitt, M. J. EPR Detection Of The Unstable *tert*-Butylperoxyl Radical Adduct of the Spin Trap 5,5-Dimethyl-1-Pyrroline *N*-Oxide: A Combined Spin-Trapping and Continuous-Flow Investigation.*J. Chem. Soc., Perkin Trans. 2*, **2002**, 2044−2051.

(26) O'Neill, P. M.; Bishop, L. P. D.; Searle, N. L.; Maggs, J. L.; Storr, R. C.; Ward, S. A.; Park, B. K.; Mabbs, F. Biomimetic Fe(II)-Mediated Degradation of Arteflene (Ro-42−1611). The First EPR Spin-Trapping Evidence for the Previously Postulated Secondary Carbon-Centered Cyclohexyl Radical. *J. Org. Chem.* **2000**, *65*, 1578−1582.

(27) Frejaville, C.; Karoui, H.; Tuccio, B.; Le Moigne, F.; Culcasi, M.; Pietri, S.; Lauricella, R.; Tordo, P. 5-(Diethoxyphosphoryl)-5-methyl-1-pyrrolidine *N*-Oxide: A New Efficient Phosphorylated Nitrone for the in Vitro and in Vivo Spin Trapping of Oxygen-Centered Radicals. *J. Med. Chem.* **1995**, *38*, 258−265.

(28) ESR@NIEHS/NIH: The Gateway to Biomedical ESR Research at http://EPR.niehs.nih.gov and references therein.

(29) Posner, G. H.; Cumming, J. N.; Ploypradith, P.; Oh, C.-H. Evidence for Fe(IV)═O in the Molecular Mechanism of Action of the Trioxane Antimalarial Artemisinin. *J. Am. Chem. Soc.* **1995**, *117*, 5885−5886. See also: Traylor, T. G.; Miksztal A. R. Mechanisms of Hemin-catalyzed Epoxidations: Electron Transfer from Alkenes. *J. Am. Chem. Soc.* **1987**, *109*, 2770−2774.

(30) (a) Kapetanaki, S.; Varotsis, C. Ferryl-Oxo Heme Intermediate in The Antimalarial Mode of Action Of Artemisinin. *FEBS Lett*. **2000**, *474*, 2/3, 238−241. (b) Kapetanaki, S.; Varotsis, C. Fourier Transform Infrared Investigation of Non-Heme Fe(III) and Fe(II) Decomposition of Artemisinin and of a Simplified Trioxane Alcohol. *J. Med. Chem.* **2001**, *44*, 3150−3156.

(31) Bhattacharjee, A. K.; Carvalho, K. A.; Opsenica, D.; Šolaja, B. A. Structure−Activity Relationship Study of Steroidal 1,2,4,5-Tetraoxane Antimalarials Using Computational Procedures. *J. Serb. Chem. Soc.* **2005**, *70*, 329−345.

(32) Wu, W. M.; Wu, Y.; Wu, Y.-L.; Yao, Z.-J.; Zhou, C.-M.; Li, Y.; Shan, F. Unified Mechanistic Framework for the Fe(II)-Induced Cleavage of Qinghaosu and Derivatives/Analogues. The First Spin-Trapping Evidence for the Previously Postulated Secondary C-4 Radical. *J. Am. Chem. Soc.* **1998**, *120*, 3316−3325.

(33) Gu, J.; Chen, K.; Jiang, H.; Leszczynski, J. The Radical Transformation in Artemisinin: A DFT Study. *J. Phys. Chem. A* **1999**, *103*, 9364−9369.

(34) Bors, W.; Michel, C.; Stettmaier, K. Radical Species Produced from the Photolytic and Pulse-radiolytic Degradation of *tert*- Butyl Hydroperoxide. An EPR Spin Trapping Investigation. *J. Chem. Soc., Perkin Trans. 2* **1992**, 1513−1517.

(35) In addition, several pathways lead to H_2O_2 expulsion; however, they do not "produce" Fe(IV)═O. These authors, based on the present knowledge in the field (See also Haynes, R. K. Reply to Comments on "Highly Antimalaria-Active Artemisinin Derivatives: Biological Activity Does Not Correlate with Chemical Reactivity". *Angew. Chem., Int. Ed*. **2005**, *44*, 2064−2065, and references therein.), would not exclude a "multiple pathways" mechanism.

(36) Svistunenko, D. A. Reaction of Haem Containing Proteins and Enzymes With Hydroperoxides: The Radical View. *Biochim. Biophys. Acta (BBA)* **2005**, *1707*, 127−155.

(37) Gordeuk, V. R.; Loyevsky, M. Iron Chelators. In *Antimalarial Chemotherapy*; Rosenthal, P. J., Ed.; Humana Press, Totowa, NJ, 2001; pp 308−309 and references therein.

(38) Sheldrick, G. M. *SHELXS-97 and SHELXL-97, Program for crystal structure refinement*; University of Göttingen: Germany, 1997.

(39) Desjardins, R. E.; Canfield, C. J.; Haynes, D. E, Chulay, J. D. Quantitative assessment of antimalarial activity in vitro by a semiautomated microdilution technique. *Antimicrob. Agents Chemother.* **1979**, *16*, 710−718.

(40) Milhous, W. K.; Weatherly, N. F.; Bowdre, J. H.; Desjardins, R. E. In vitro activities of and mechanisms of resistance to antifol antimalarial drugs. *Antimicrob. Agents Chemother.* **1985**, *27*, 525−530.

JM050966R